

# Nanoporous Silica Grown in Organic Media: Absorption and NMR Characterization

Roberto Simonutti, Angiolina Comotti, Silvia Bracco, Alessandra Simonelli, and Piero Sozzani\*

Department of Materials Science and INSTM, Milan-Bicocca Research Unit,  
University of Milan-Bicocca, via R. Cozzi 53, I-20125 Milan, Italy

Received March 21, 2002. Revised Manuscript Received May 23, 2002

Pure silica of high surface area was prepared by the slow evaporation of colloidal solutions of silicic acid in organic solvents. The porous silica materials were characterized by nitrogen adsorption, adsorption of volatile organic molecules, and  $^{29}\text{Si}$  magic angle spinning (MAS) NMR. The absorption properties and the high concentration of silanols, detected by  $^{29}\text{Si}$  NMR resonances, are consistent with a surface area of 600–700  $\text{m}^2/\text{g}$ . The high surface area and the virtual lack of long-range order suggest the model of a “sponge” containing open and interconnected pores. The size of the pores or channels is relatively homogeneous and is affected quite markedly by the organic preparation medium. The pores of the structure obtained using tetrahydrofuran are on the subnanometer scale, an indication that the diffusive phenomena must be influenced by intimate organic–inorganic interactions during the slow evaporation of the solvent.

## Introduction

New synthetic routes have stimulated the preparation of a wide variety of microporous and mesoporous materials, the pore sizes of which were tailored from a few angstroms to several nanometers.<sup>1</sup> Such systems provide extended and well-defined interfaces that are ideal for the production of nanocomposites with unprecedented properties.<sup>2</sup> In fact, a molecule confined to a restricted environment on the nanometer scale shows completely different conformational and dynamical behavior from that of the same molecule in the bulk phase. The unusual properties of single elongated molecules and polymer chains surrounded by cylindrical crystalline nanochannels have been described by our group.<sup>3</sup> On considering amorphous inorganic matrixes, the best known example is, perhaps, that of polymers included in the pores of Vycor glass,<sup>4</sup> where the average pore dimension (30–70 Å) has a relevant effect on the radii of gyration of the chains.<sup>5</sup> Several other examples of scientific and practical interest can be found in the literature; these include composites with improved mechanical properties, such as organo-modified fello-silicates,<sup>6</sup> which are prepared by taking advantage of

the absorption of polymers in the galleries and cavities of porous fillers.

In Vycor glass, the mesopores have a complex tubular network geometry due to the preparation process, which is based on the spinodal decomposition of borosilicate mixtures.<sup>7</sup> In fact, at high temperature, the borosilicate phase separates at the microscopic level into two continuous phases, one rich in silica and the other, in borosilicate and alkali. Acid leaching then removes the borosilicate phase, and accessible pores are produced.

High surface area silica materials can be prepared by sol–gel techniques starting from silicon alkoxides. The hydrolysis of tetramethoxysilane or tetraethoxysilane under well-defined conditions can lead to the formation of a gel, and the subsequent drying of the gel by evaporation (xerogel) or supercritical extraction (aerogel) can produce porous materials of very low density.<sup>8</sup>

A template mechanism can be used to prepare mesoporous silica-based materials possessing a uniform hexagonal array of cylindrical mesopores (MCM-41).<sup>9</sup> The pore structure is due to the cooperative organization of silicate and surfactant species in water coupled with inorganic polymerization.<sup>10</sup> By removing the templating molecules by calcination, accessible regular channels of a few nanometers in diameter are obtained, the actual

\* Corresponding author. E-mail: piero.sozzani@mater.unimib.it.

(1) Corma, A. *Chem. Rev.* **1997**, *97*, 2373.

(2) *Chem. Mater.* **2001**, *10* (Organic–Inorganic Nanocomposite Materials, special issue).

(3) (a) Sozzani, P.; Bovey, F. A.; Schilling, F. C. *Macromolecules* **1989**, *22*, 4225. (b) Sozzani, P.; Behling, R. W.; Schilling, F. C.; Bruckner, S.; Helfand, E.; Bovey, F. A.; Jelinski, L. W. *Macromolecules* **1989**, *22*, 3318. (c) Sozzani, P.; Bovey, F. A.; Schilling, F. C. *Macromolecules* **1991**, *24*, 6764. (d) Sozzani, P.; Amundson, K. R.; Schilling, F. C. *Macromolecules* **1994**, *27*, 6498. (e) Sozzani, P.; Simonutti, R.; Comotti, A. *Mol. Cryst. Liq. Cryst.* **1996**, *277*, 299. (f) Comotti, A.; Simonutti, R.; Catel, G.; Sozzani, P. *Chem. Mater.* **1999**, *11*, 1476.

(4) Mirau, P. A.; Heffner, S. A.; Schilling, M. *Chem. Phys. Lett.* **1999**, *313*, 139.

(5) Lal, J.; Sinha, S. K.; Auvray, L. *J. Phys. II France* **1997**, *7*, 1597.

(6) (a) LeBaron, P. C.; Pinnavaia, T. J. *Chem. Mater.* **2001**, *13*, 3760. (b) Shi, H. Z.; Lan, T.; Pinnavaia, T. J. *Chem. Mater.* **1996**, *8*, 1584. (c) Giannelis, E. P. *Adv. Mater.* **1996**, *8*, 29.

(7) Hood, H. P.; Nordberg, M. E. U.S. Patent 2,106,744, 1938 and U.S. Patent 2,286,275, 1942.

(8) Brinker, C. J.; Scherer, G. W. *Sol–Gel Science*; Academic Press: San Diego, CA, 1990.

(9) Kresge, C. T.; Leonowics, M. E.; Roth, W. J.; Vartuli, J. C.; Beck, J. S. *Nature (London)* **1992**, *359*, 710.

(10) Huo, Q.; Margolese, D. I.; Ciesla, U.; Demuth, D. G.; Feng, P.; Gier, T. E.; Sieger, P.; Firouzi, A.; Chmelka, B. F.; Schüth, F.; Stucky, G. D. *Chem. Mater.* **1994**, *6*, 1176.

diameter depending on the chain length of the templating agent.<sup>11</sup>

In the present paper, we took an alternative route to preparing silica of high surface area by evaporating a colloidal solution of silicic acid in an organic solvent. It has been reported that after the acidification of an aqueous silicate solution an organic solvent can extract silicic acid in reasonable yield.<sup>12</sup> Furthermore, it has been stated that silicic acid is quite stable in organic solvents at relatively low concentration and is able to undergo silylation and esterification reactions.<sup>13</sup> However, there was no characterization of the material directly obtained by condensation of silicic acid in the organic medium. The characterization of the structure and the physicochemical properties of the highly porous materials that were eventually obtained are examined in this paper.

Inorganic materials with extended interfaces, obtained in organic media, are of specific interest because the growth of the hybrid interfaces may be effective in forming nanocomposites with hydrocarbon polymers because of the advantage of operating in mutually compatible organic media. Actually, nanocomposites between hydrophilic polymers, or polymers modified by polar groups and silicates, are easily prepared, but the effective dispersion of silica or silicates in hydrocarbon polymers at the nanometer level is still a challenge.

### Experimental Section

**Synthesis.** Silica was synthesized starting from anhydrous sodium metasilicate  $\text{Na}_2\text{SiO}_3$  (97%, Fluka). The extraction of silicic acid with organic solvents was carried out as follows: 6.4 g of inorganic precursor dissolved in 50 mL of deionized water was added dropwise (3 mL/min) to 50 mL of aqueous hydrochloric acid (2.5 M) under moderate magnetic stirring at 0 °C. After a few minutes, keeping the same temperature and stirring speed, 100 mL of organic solvent was added dropwise (4.5 mL/min). After complete solvent addition, the solution, which is homogeneous, was stirred for 1 h. To separate the organic phase containing the silicic acid and the aqueous phase, 30 g of NaCl was added. The solvents used were tetrahydrofuran (THF), 2-propanol (IPA), acetone, xylene, chloroform, methylene chloride, methanol, and ethanol.

**Nitrogen Adsorption.** Nitrogen adsorption-desorption isotherms were measured at liquid nitrogen temperature using a Coulter SA 3100 analyzer. The samples were outgassed for 2 h at 100 °C. Surface area was calculated using the Brunauer, Emmet, and Teller (BET model).<sup>14</sup> In the case of mesoporosity, the pore-size distributions were evaluated following the method developed by Barret, Joyner, and Halenda (BJH model).<sup>15</sup>

**Absorption Measurements.** The absorption of benzene was measured using a gas absorption manometry apparatus.<sup>16</sup> The samples were outgassed overnight at 100 °C. Absorption equilibrium was normally reached in less than 30 min. The measurements were carried out at room temperature and in the range of pressure where the vapor phases behave as ideal gases.

**Solid-State NMR.** Nuclear magnetic resonance (NMR) high-resolution <sup>29</sup>Si magic angle spinning (MAS) spectra were run at 59.6 MHz on an AVANCE 300 Bruker instrument operating at a static field of 7.04 T. A MAS Bruker probe was used with 7-mm  $\text{ZrO}_2$  rotors; the spinning speed ranged between 2 and 4.5 kHz. The experiments were made using high-power proton decoupling (DD). <sup>29</sup>Si cross polarization (CP) MAS experiments were run using a 90° pulse of 6 μs with a delay time of 10 s, and 800–1000 scans were collected (proton decoupling field of 42 kHz). Quantitative <sup>29</sup>Si single-pulse excitation (SPE) MAS experiments were recorded using a recycle delay of 100 s, and 2000–3000 scans were collected. The resolution for silicon was checked on a  $\text{Q}_8\text{M}_8$  sample (trimethylsilylester of octameric silicic acid,  $\text{Si}_8\text{O}_{20}\text{H}_8$ ). The  $\text{Q}_8\text{M}_8$  sample was also used as a second standard by assigning the <sup>29</sup>Si chemical shift of the trimethylsilyl groups to +11.5 ppm from TMS.<sup>17</sup>

### Results and Discussion

The silica samples are obtained from solutions of silicic acid in THF and from solutions of silicic acid in IPA, which are solvents that extract silicic acid in the highest yield. Once the silicic acid has been extracted, 10 mL of solution is transferred in a Teflon vessel, the vessel is then sealed by Parafilm, and a few pinholes are made to allow gentle evaporation of the solvent. The physical aspect of the obtained silica samples is that of platelets. The samples were ground and washed repeatedly with deionized water to remove soluble species such as NaCl or uncondensed silicic acid.

Figure 1 shows the absorption-desorption nitrogen isotherms for silica obtained from IPA and THF, whereas Table 1 reports the calculations carried out together with the yields of obtained material. Apolar solvents such as xylene do not extract appreciable amounts of silicic acid; solvents such as ethanol do not demix even after increasing the ionic strength of the aqueous solution considerably. The silica obtained from THF (Figure 1b) shows the peculiar features of a microporous system: the isotherm, concave to the pressure axis, rises sharply at low pressure and reaches a plateau. This behavior is defined as Type I, following IUPAC classification. The narrow range of relative pressure needed to reach a plateau is due to the presence of small pores with sizes in the nanometer range; furthermore, a horizontal plateau indicates a rather small external surface area. The surface area, according to the BET model, is 616 m<sup>2</sup>/g. The silica from IPA shows different behavior (Figure 1a): at low relative pressure, the isotherm is concave, but above 0.1 P/P<sup>0</sup>, it becomes linear and finally levels off at P/P<sup>0</sup> higher than 0.8. In this case, there is a multilayer formation. A broad triangular hysteresis loop is observed at relative pressures above ca. 0.5. Some features of this isotherm correspond to those of the Type IV isotherm, but the absence of a clear step on its adsorption branch indicates a nonuniform porous system. In this case, it is reasonable to apply the methodology developed by Barret, Joyner, and Halenda to the desorption isotherm branch (BJH);<sup>15</sup> the pore-size distribution that is obtained is reported in Figure 2. The distribution is centered around 5 nm, and there is no evidence of macropores. The surface area, according to the BET model, is 623 m<sup>2</sup>/g.

The porosity of the silica samples obtained from silicic acid in organic solvents is also confirmed by the benzene

(11) Simonutti, R.; Comotti, A.; Bracco, S.; Sozzani, P. *Chem. Mater.* **2001**, *13*, 771.

(12) Abe, Y.; Sekiguchi, T.; Misono, T. *J. Polym. Sci., Polym. Chem. Ed.* **1984**, *22*, 761.

(13) Abe, Y.; Misono, T. *J. Polym. Sci., Polym. Lett. Ed.* **1984**, *22*, 565.

(14) Brunauer, S.; Emmett, P. H.; Teller, E. *J. Am. Chem. Soc.* **1938**, *60*, 309.

(15) Barret, E. P.; Joyner, L. G.; Halenda, P. P. *J. Am. Chem. Soc.* **1951**, *73*, 373.

(16) Rouquerol, F.; Rouquerol, J.; Sing, K. *Adsorption by Powders and Porous Solids*; Academic Press: London, 1999; p 53.

(17) Sindorf, D. W.; Maciel, G. E. *J. Am. Chem. Soc.* **1983**, *105*, 1487.

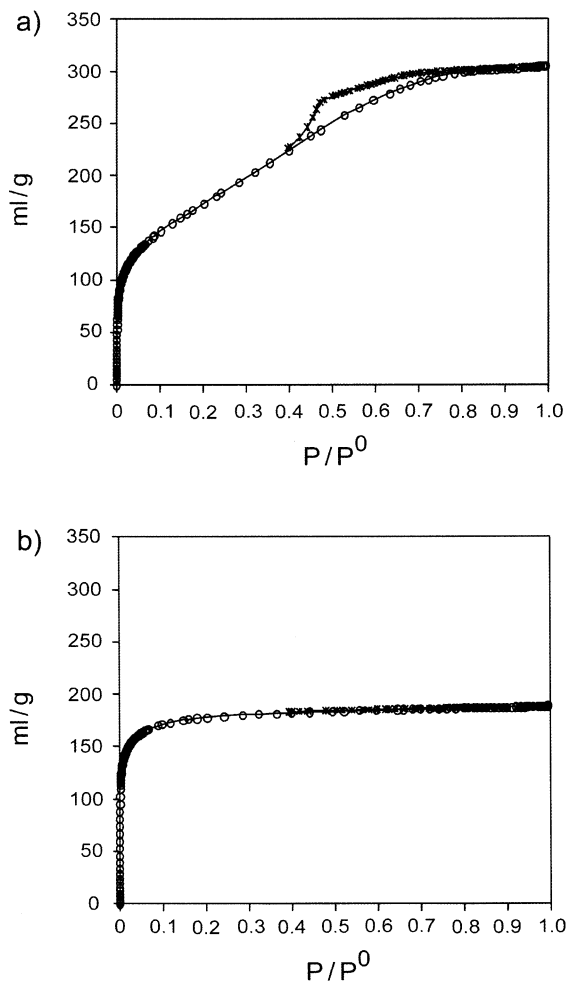


**Figure 1.** (a)  $N_2$  sorption isotherms of silica condensed in IPA. (b)  $N_2$  sorption isotherms of silica condensed in THF. The isotherms were measured at 77 K.

**Table 1. Yield of Silicic Acid Extraction in Various Solvents (Measured as Dry Silica) and Surface Area of the Obtained Silica**

| organic solvent                | extracted silica, g/L | surface area, $m^2/g$ |
|--------------------------------|-----------------------|-----------------------|
| THF                            | 36                    | 616                   |
| IPA                            | 38                    | 623                   |
| acetone                        | 21                    | 205                   |
| "apolar" solvents <sup>a</sup> | no extraction         |                       |
| polar solvents <sup>b</sup>    | no demixing           |                       |

<sup>a</sup> Xylene, chloroform, methylene chloride. <sup>b</sup> Ethanol, methanol.

sorption capacity. Figure 3 allows a comparison of the benzene sorption isotherms of silica obtained from IPA, THF, and acetone with that of commercial precipitated silica (VN3 from Degussa with specific surface area of  $170 m^2/g$ ) to be made. The IPA, THF, and acetone silica samples have sorption capacities of 0.25, 0.15, and 0.13 mol/mol, respectively, that lie between the extremely high value of the reference mesoporous MCM-41 sample (0.5 mol/mol) and the low value of commercial silica. The pattern followed by the acetone sample is similar to that of the IPA sample, although it has a less efficient absorption capacity. Also, for benzene sorption, the silica from THF shows microporous system behavior because the isotherm reaches the plateau value at very low relative pressure.

Small-angle powder X-ray diffraction has been carried out on silica obtained from THF and IPA solutions; in

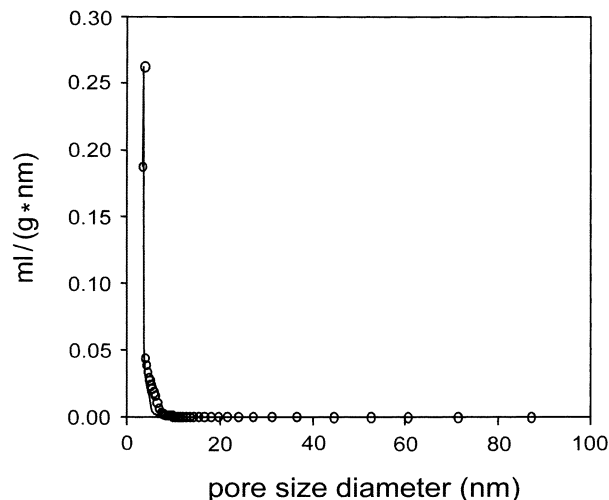


**Figure 2.** Pore-size distribution of silica from IPA obtained by applying the BJH method.

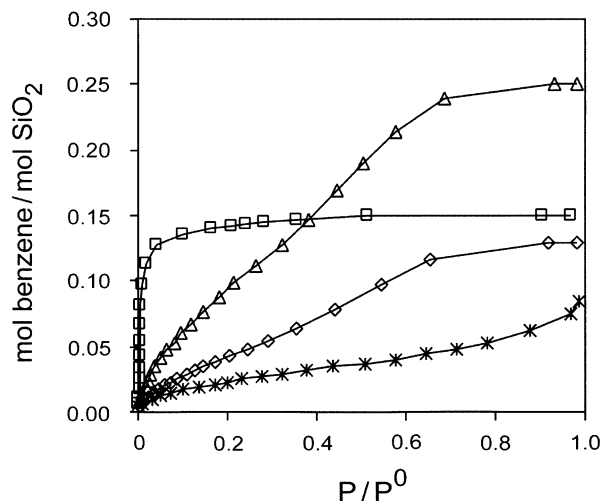


**Figure 3.** Benzene sorption isotherms of silica obtained from THF ( $\square$ ), IPA ( $\Delta$ ), silica gel VN3 ( $\times$ ), and acetone ( $\diamond$ ). The measurements were made at room temperature.

both cases, there is no evidence of long-range order. In fact, SAXS patterns show only a broad peak centered around a  $2\theta$  value of  $1.5^\circ$  (not shown).

$^{29}Si$  solid-state NMR techniques provide valuable information about silica structure and morphology.<sup>18</sup>  $^{29}Si$  CPMAS NMR spectra can describe the silica surface by quantifying the silicon species that receive magnetization from silanols and water protons. Silicon atoms bearing two hydroxyl groups,  $(Si-O)_2Si-(OH)_2$  (called  $Q^2$ ), have a chemical shift (CS) of  $-89$  ppm, whereas silicon atoms bearing one hydroxyl group,  $(Si-O)_3Si-OH$  (called  $Q^3$ ) resonate at  $-99$  ppm. Both silicon types, located mainly at the surface, are quite close to protons and can cross polarize efficiently. Silicon atoms without hydroxyl groups,  $Si(Si-O)_4$  (called  $Q^4$ ), with a CS of  $-109$  ppm, constitute the bulk of the silica particles, and only a small portion of them are near the surface

(18) (a) Maciel, G. E.; Sindorf, D. W. *J. Am. Chem. Soc.* **1980**, *102*, 7607. (b) Sindorf, D. W.; Maciel, G. E. *J. Am. Chem. Soc.* **1981**, *103*, 4263. (c) Sindorf, D. W.; Maciel, G. E. *J. Phys. Chem.* **1982**, *86*, 5208. (d) Pfeiderer, B.; Albert, K.; Bayer, E.; van de Ven, L.; de Haan, J.; Cramers, C. *J. Phys. Chem.* **1990**, *94*, 4189. (e) Leonardelli, S.; Facchini, L.; Fretigny, C.; Tougne, P.; Legrand, A. P. *J. Am. Chem. Soc.* **1992**, *114*, 6412.



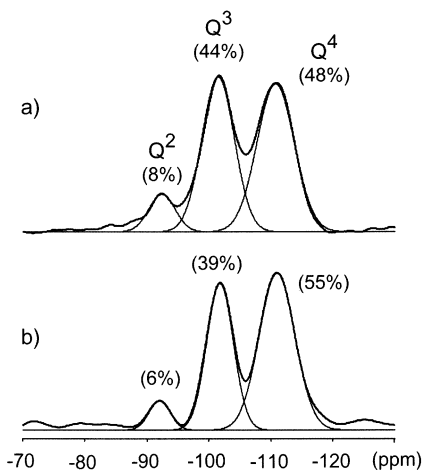


**Figure 4.** 59.6 MHz  $^{29}\text{Si}$  SPE MAS NMR (recycle delay of 100 seconds) spectra of (a) silica obtained from THF and (b) silica obtained from IPA. The spectra were fully deconvoluted by Gaussian line shapes, and the single lines are reported for  $\text{Q}^2$  at  $-89$  ppm,  $\text{Q}^3$  at  $-99$  ppm, and  $\text{Q}^4$  at  $-109$  ppm. The percentage of the  $\text{Q}^2$ ,  $\text{Q}^3$ , and  $\text{Q}^4$  species are reported in parentheses.

and are able to receive proton magnetization.<sup>18</sup> Therefore, the CPMAS NMR spectrum, especially for short contact times, describes the silica surface, whereas the  $^{29}\text{Si}$  MAS NMR spectrum without CP and with long recycle delays quantitatively describes the structure of the silica particles.<sup>19</sup> By this procedure, the quantification of  $\text{Q}^n$  species is affected by an error less than  $\pm 5\%$ .

Figure 4 shows the  $^{29}\text{Si}$  MAS NMR spectra (recycle delay of 100 s) of the silica obtained from THF and IPA, and the three broad peaks due to the  $\text{Q}^2$ ,  $\text{Q}^3$ , and  $\text{Q}^4$  species provide the benchmark of amorphous silica. The peculiar feature of the spectra lies in the exceptionally intense  $\text{Q}^3$  resonance, the  $\text{Q}^3$  and  $\text{Q}^4$  signals being of comparable intensity; the  $^{29}\text{Si}$  MAS NMR spectra of precipitated silica usually show a  $\text{Q}^4$  peak that is almost twice as large as the  $\text{Q}^3$  peak. Also, pyrogenic silica presents a large  $\text{Q}^4$  resonance compared to that of  $\text{Q}^3$ , though the synthesis at high temperature and the rapid cooling of the particles cause highly strained Si–O–Si bond angles with a spreading out of the chemical shifts.<sup>20</sup>

To find systems with such high  $\text{Q}^3/\text{Q}^4$  ratios, high surface-silica materials such as mesoporous MCM-41 or SBA-1 must be taken into account. Globular or cylindrical micelles tend to act as casts for the soluble silicate species, and silicate condensation leads to the formation of mesophases with intriguing geometry (lamellar, cubic, or hexagonal). The relatively narrow walls, compared to the pore dimensions, bring about a high  $\text{Q}^3$  species content, compared to that of  $\text{Q}^4$ . Once calcined, these systems show very high surface areas (higher than 1000  $\text{m}^2/\text{g}$ ). The  $\text{N}_2$  isotherms for cubic and hexagonal structures of MCM-41 belong to Type IV and show capillary condensation.

The  $^1\text{H}$  to  $^{29}\text{Si}$  cross polarization technique relies on strong dipolar coupling between silicon atoms and protons; therefore, in CPMAS NMR spectra, the signals due to  $\text{Q}^2$  and  $\text{Q}^3$  are enhanced, and those related to  $\text{Q}^4$

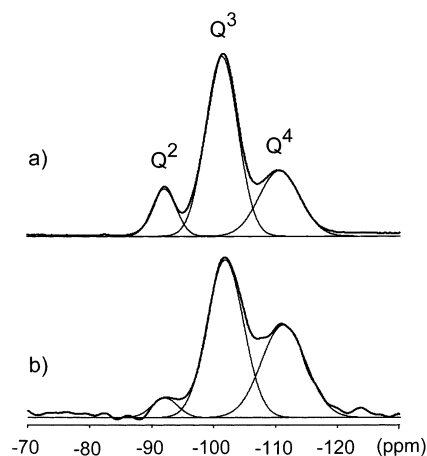


**Figure 5.** 59.6 MHz  $^{29}\text{Si}$  CPMAS NMR spectra of (a) silica obtained from THF and (b) silica obtained from IPA. The spectra were fully deconvoluted by Gaussian line shapes, and the single lines are reported for  $\text{Q}^2$  at  $-89$  ppm,  $\text{Q}^3$  at  $-99$  ppm, and  $\text{Q}^4$  at  $-109$  ppm. The contact time of 3 ms is applied.

tend to be reduced.<sup>18</sup> In fact, the closest proton to  $\text{Q}^2$  or  $\text{Q}^3$  is two bonds away, whereas the closest to a  $\text{Q}^4$  atom is at least four bonds away; moreover,  $\text{Q}^4$  atoms are mainly present in the bulk of the silica particles and are quite far from the protons.  $\text{Q}^2$  and  $\text{Q}^3$  can be present at the silica surface but not in the bulk; therefore,  $^1\text{H}$  to  $^{29}\text{Si}$  CPMAS NMR spectra give a good description of the silica surface. Figure 5 shows the  $^{29}\text{Si}$  CPMAS NMR spectra of the silica obtained from THF and IPA; the traces are comparable to those of high surface-silica samples. The  $\text{Q}^3/\text{Q}^4$  ratio is higher in the silica obtained from THF, and the  $\text{Q}^2$  peak is also sharper and better defined. This behavior is relatively unusual in amorphous silica; in fact, both silica gels and precipitated silica show poorly resolved  $\text{Q}^2$  peaks. The quite low percentage of the  $\text{Q}^2$  signal in the system obtained from IPA describes a relatively even surface. As reported by Maciel et al.,<sup>21</sup> a complex model of intersecting (100)-type and (111)-type  $\beta$ -cristobalite faces can be used to describe the silica surface, where the (100)-type faces present only  $\text{Q}^2$  species and the (111)-type faces, only  $\text{Q}^3$ . Increasing the amount of  $\text{Q}^2$  results in a more frequent occurrence of intersections, indicating a more corrugated surface.

Silica obtained with organic solvent extraction shows behavior that is between that of nonstructured precipitated or pyrogenic silica and structured mesoporous silica.<sup>9</sup> The high  $\text{Q}^3/\text{Q}^4$  ratio is a clear indication of the low degree of silica condensation, which is probably due to the presence of the polar solvent. After extraction, the silicic acid starts polymerizing slowly in the organic environment, and the process is accelerated by solvent evaporation. During the final evaporation stages, the organic component is trapped in the silica matrix and can act as a cast for the silica. The different interactions of the silica species with THF and IPA can explain the type of porosity obtained from case to case. Similar template effects with small molecules have been reported in the synthesis of mesoporous silica. For example, nonsurfactant molecules such as glucose and urea have been employed as templates or pore-forming agents in aqueous solutions.<sup>22</sup>

(19) Fyfe, C. A.; Gobbi, G. C.; Kennedy, G. C. *J. Phys. Chem.* **1985**, *89*, 277.

(20) Liu, C. C.; Maciel, G. E. *J. Am. Chem. Soc.* **1996**, *118*, 5103.

(21) Chuang, I.-S.; Maciel, G. E. *J. Am. Chem. Soc.* **1996**, *118*, 401.

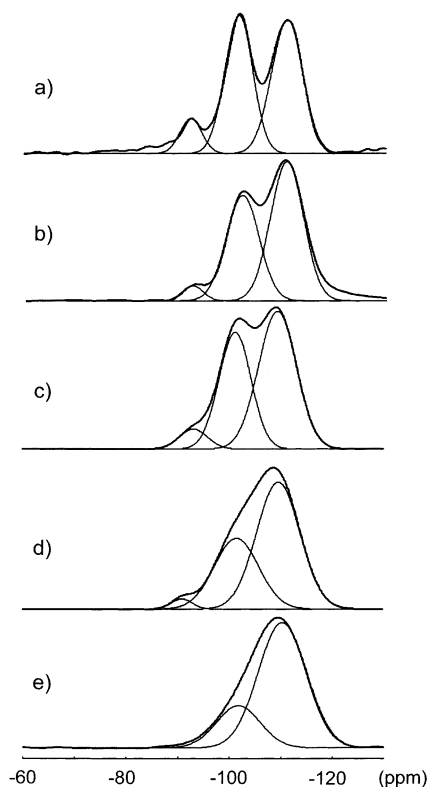


**Figure 6.** 59.6 MHz  $^{29}\text{Si}$  SPE MAS NMR spectra of silica obtained from THF treated at the reported temperatures for 4 h: (a) untreated, (b) 120 °C, (c) 200 °C, (d) 450 °C, and (e) 750 °C. Spectra were fully deconvoluted by Gaussian line shapes, and the single lines are reported for  $\text{Q}^2$  at -89 ppm,  $\text{Q}^3$  at -99 ppm, and  $\text{Q}^4$  at -109 ppm.

**Table 2.** Line Width at Half Height (LW) and Signal Area Percentage of the  $\text{Q}^2$ ,  $\text{Q}^3$ , and  $\text{Q}^4$  Species for the Silica Obtained from THF Treated at the Reported Temperatures

| thermal treatment | $\text{Q}^2$            |                        | $\text{Q}^3$            |                        | $\text{Q}^4$            |                        |
|-------------------|-------------------------|------------------------|-------------------------|------------------------|-------------------------|------------------------|
|                   | area, <sup>a</sup><br>% | LW, <sup>b</sup><br>Hz | area, <sup>a</sup><br>% | LW, <sup>b</sup><br>Hz | area, <sup>a</sup><br>% | LW, <sup>b</sup><br>Hz |
| none              | 8                       | 298                    | 44                      | 380                    | 48                      | 423                    |
| 4 h at 120 °C     | 4                       | 280                    | 41                      | 447                    | 55                      | 456                    |
| 4 h at 200 °C     | 6                       | 386                    | 39                      | 434                    | 55                      | 512                    |
| 4 h at 450 °C     | 2                       | 280                    | 36                      | 602                    | 62                      | 588                    |
| 4 h at 750 °C     |                         |                        | 24                      | 630                    | 76                      | 647                    |

<sup>a</sup> Areas were determined from the deconvolution of the peaks of  $^{29}\text{Si}$  SPE MAS NMR spectra. The error in the evaluation of the peak areas can be estimated as  $\pm 5\%$  of the measured values ( $\pm 10\%$  in the case of the sample treated for 4 h at 750 °C). <sup>b</sup> Estimated error in the determination of the LWs is less than  $\pm 5\%$ .

The thermal behavior of the material was followed by recording the  $^{29}\text{Si}$  MAS NMR spectra of silica samples from THF (with long recycle delays) held at 120, 200, 450, and 750 °C for 4 h under nitrogen. Figure 6 shows the relative spectra, and Table 2, the results of deconvolution. The  $\text{Q}^3/\text{Q}^4$  ratio does not change significantly until treatment at 450 °C, although it becomes evident that the signals are broader. At 450 °C, the condensation of the silanols proceeds further, especially on the surface, causing a decrease in the  $\text{Q}^3$  species in favor of the  $\text{Q}^4$ . Only after the treatment at 750 °C does the  $\text{Q}^3/\text{Q}^4$  ratio becomes similar to that of precipitated

silicas, indicating a partial collapse of the pore structure. The increase of the  $\text{Q}^3$  and  $\text{Q}^4$  line widths with thermal treatment is an indication that the condensation of the silanols causes shrinkage of the pores. The local distortion of the siloxanic tetrahedra correlated with the shrinkage is an effective source of inhomogeneous broadening.<sup>23</sup>

## Conclusions

Novel microporous materials obtained by the condensation of silica in organic media were characterized by adsorption techniques and MAS NMR spectroscopy. The suggested model is that of a material with the structure of a sponge containing open nanochannels. The absorption capacity and the surface area (600–700  $\text{m}^2/\text{g}$ ) are considerable. The pore, or channel, size is relatively homogeneous and is affected markedly by the organic medium used during preparation. A strong link between the cast medium and the structure of the porous material supports the existence of template structures as intermediates, which are formed by the inorganic condensate and the organic molecules. The imprinting effect of the cast medium, demonstrated here, could be exploited as a novel tool for fine-tuning porosity.

The large number of nanometer-size pores present in the silica grown in organic solvents and the possibility of obtaining films of different thicknesses by varying the quantity of solution used make the methodology presented in this paper particularly suited for the preparation of insulators with a low dielectric constant ( $k$ ). In fact, the presence of air inside the voids ( $k = 1$ ) can decrease the  $k$  of silica ( $k = 4\text{--}4.2$ ) depending on the fraction and connectivity of the pores. The peculiar properties of this type of silica can also lead to applications in the development of detectors and sensors. In fact, the uptake of benzene, especially at low partial pressure, is quite remarkable compared to that of commercially available silicas.

The feasibility of condensing silica “in situ” from organic media can open novel routes to the preparation of polymer nanocomposites and reinforced hydrocarbon polymers. THF, for example, is a good polymer solvent, and thus it is possible to have a homogeneous solution containing both the polymer and the silica precursor. Once the solvent has been removed, an intimate composite is more likely produced than when using pre-formed silica particles. Finally, the fact that the inorganic precursors (sodium silicates) are available at low cost is a great incentive toward using such silica grown in organic media for the aforementioned applications.

**Acknowledgment.** Financial support from MIUR (PRIN program) and CNR PF MSTAII is gratefully acknowledged. We thank Dr. F. Negroni for helpful discussions and Professor A. Marigo for the SAXS measurements. A.S. thanks Pirelli Spa for the Ph.D. scholarship.

CM0211709

(22) Wei, Y.; Xu, J.; Dong, H.; Dong, J. H.; Qiu, K.; Jansen-Varnum, S. A. *Chem. Mater.* **1999**, *11*, 2023.

(23) Simonutti, R.; Comotti, A.; Negroni, F.; Sozzani, P. *Chem. Mater.* **1999**, *11*, 822.